Electrostatic Fiber Spinning from Polymer Melts. III. Electrostatic Deformation of a Pendant Drop of Polymer Melt

L. LARRONDO and R. ST. JOHN MANLEY, *Pulp and Paper Research Institute of Canada, Montreal, Quebec, Canada H3A 2A7 and Department of Chemistry, McGill University, Montreal, Quebec, Canada H3A 2A7*

Synopsis

It has been previously shown that fine jets can be drawn from polymer melts with the aid of an electric field. In an effort to understand the mechanism of jet formation, preliminary experiments have been carried out on the deformation of pendant drops of molten polymers (nylon 12 and polyethylene) subjected to an electric field. The drop deformation was measured as a function of field intensity and frequency, and the results were interpreted in terms of a theory due to Torza et al. It is shown that there is qualitative agreement between the theory and experimental observations. This permits the identification of the parameters influencing the drop deformation and leads to a qualitative picture of the mechanism of deformation.

INTRODUCTION

It has been known for many years that the horizontal free surface of a monomeric liquid in a vertical electrical field can become unstable, resulting in the formation of vertical jets of liquid if the field intensity is sufficiently large. Several authors have described experiments with such jets.[1-12]

It has been shown elsewhere[13] that this phenomenon is also exhibited by polymer melts. Continuous filaments of rapidly crystallizing polymers, such as polyethylene and polypropylene, were spun from the melt using an electrical field as the only driving force. The polymer melt was fed into a metallic capillary forming a hemispherical drop at the end of the orifice. An electrical field was applied between the orifice and a conducting plate held perpendicular to the axis of the orifice. Above a critical field intensity a steady jet of molten polymer was drawn, rapid solidification ensued due to crystallization and a continuous filament was formed.

At present a rational description of the mechanics of these electrically driven jets does not exist. Taylor[1] subjected the phenomenon to a theoretical treatment but was unable to go much beyond a calculation of the force which the electric field exerts on the fluid. The experiments to be described here were undertaken in the hope of furthering our understanding of the mechanism of jet formation with particular reference to polymer melts. More specifically, we wish to investigate whether existing theories can describe the electrostatic deformation of highly viscous and elastic polymer melts.

For this purpose we have measured the deformation of hemispherical drops of polymer melt in an electric field and interpreted the results in terms of a theory due to Torza, Cox, and Mason.[14] The measurements were made in the experi-

mental arrangement described above in order to closely approximate the conditions in electrostatic fiber spinning. The theory, however, was developed for the specific case of a spherical liquid drop suspended in an immiscible liquid, subject to a uniform electric field. Nevertheless, it will be seen that this theory gives an adequate description of the experimental observations and, in addition, some points of interest have emerged from these considerations.

THEORETICAL

In order to facilitate subsequent discussion the salient features of the theory due to Torza et al.[14] are briefly reviewed in this section.

A drop of radius b which carries no net electric charge is suspended in an immiscible liquid subject to a uniform electric field whose strength E, far from the drop, varies with time according to

$$E = E_0 \cos\omega t \tag{1}$$

where $\omega = 2\pi\nu$ is the angular frequency of the field and E_0 is the peak value of the field when $\nu > 0$ and the steady value when $\nu = 0$. It is assumed that the dielectric constants K_1 and K_2, and the Ohmic resistivities χ_1 and χ_2, of the drop and medium, respectively, are independent of ν. The center of the drop is taken as the origin of the polar coordinates r, θ.

The resultant charge density σ on the drop surface is given by

$$\sigma = \frac{3\epsilon_0 K_2 E_0(1 - Rq)\cos\theta}{[(2R + 1)^2 + a^2\omega^2(q + 2)^2]^{1/2}} \cos(\omega t - \alpha_\nu) \tag{2}$$

where

$$\alpha_\nu = \tan^{-1}\left(\frac{a\omega(q + 2)}{2R + 1}\right), \qquad 0 < \alpha_\nu < \pi/2$$

and

$$R = \chi_1/\chi_2, \qquad q = K_1/K_2, \qquad a = \epsilon_0 K_2 \chi_1$$

ϵ_0 is the permittivity of free space, which in the mks system (SI) of units is equal to 8.85×10^{-12} F m^{-1}.

Equation (2) shows that σ decreases with increasing frequency when all the other parameters are fixed; that the drop hemisphere facing the positive electrode becomes positively charged and that facing the negative electrode becomes negatively charged for $Rq > 1$ and vice versa for $Rq < 1$; when $Rq = 1$, $\sigma = 0$ over the whole surface (see Fig. 1).

In what follows, it is assumed that the suspending medium is a perfect dielectric, so that only normal electrical stresses account for the induced deformation. Furthermore, because of the high viscosity of the drops used in the present experiment, time-dependent electrical stresses can be considered to be negligible[15]; accordingly, only steady deformations are considered.

The deformation of the drop results from normal electrical stresses developed on the interface, which are balanced by the interfacial tension. To balance the electrical stresses $f_{n\nu}$, changes in the curvature of the drop surface must satisfy the Young–Laplace capillarity equation in the form

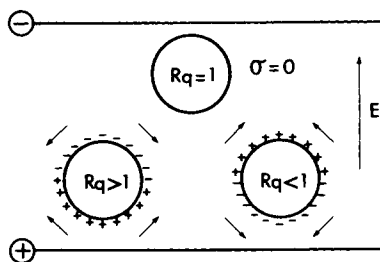$$f_{n\nu} = \gamma(b_1^{-1} + b_2^{-1}) \tag{3}$$

Fig. 1. Schematic representation of drops in an electric field E showing the charge distribution for various values of the product Rq. The arrows indicate the mode of deformation which gives rise to oblate ($Rq > 1$) or prolate ($Rq < 1$) spheroids.

where b_1 and b_2 are the principal radii of curvature at any point on the deformed drop surface and γ is the interfacial tension. Thus, with a knowledge of the electrical stresses $f_{n\nu}$, the steady electrical deformation can be calculated and is given by

$$D_\nu = (9\epsilon_0 K_2/16\gamma)\phi_\nu(\overline{E}_0^2 b) = m_\nu(\overline{E}_0^2 b) \tag{4}$$

where

$\phi_\nu =$

$$1 - \frac{R(11\lambda + 14) + R^2[15(\lambda + 1) + q(19\lambda + 16)] + 15a^2\omega^2(1 + \lambda)(1 + 2q)}{5(1 + \lambda)\left[(2R + 1)^2 + a^2\omega^2(q + 2)^2\right]} \tag{5}$$

and where λ is the ratio of the viscosity μ_1 of the drop and μ_2 of the medium. It may be noted that by using $\overline{E}_0$, the case $\nu = 0$ is included in eq. (4).[14]

ϕ_ν as defined by eq. (5) is a discriminating function which determines the type of deformation: the drop becomes a prolate spheroid ($D_\nu > 0$) when $\phi_\nu > 0$, and an oblate spheroid ($D_\nu < 0$) when $\phi_\nu < 0$.

It follows from eqs. (4) and (5) that (i) when $Rq > 1$,

$$\partial D_\nu/\partial\nu > 0 \tag{6}$$

the deformation increases with frequency, and vice versa for $Rq < 1$, and (ii) when $Rq = 1$ the deformation D_ν is independent of the frequency.

In an experimental investigation using systems of simple liquids, Torza, Cox, and Mason verified the predictions of eq. (4) but found measured deformations that were generally greater than the corresponding theoretical values. Several reasons for the discrepancy were suggested and will be mentioned briefly below.

EXPERIMENTAL

The polymers used were polyethylene (Marlex 6009) and nylon 12 at temperatures of 200 and 220°C, respectively. The electrical properties, as well as the surface tension of the polymers were taken as those reported in the literature.[16-20] The relevant parameters are listed in Table I.

The experiments were performed in the apparatus described in detail elsewhere.[13] Essentially, the polymer melt was fed from a reservoir into a conducting capillary, at the end of which a hemispherical drop was formed. The dimensions of the capillary were 0.22 cm internal diameter (D), 0.6 cm external diameter,

TABLE I
Properties of the Polymers

Phase 1[a]	M_w	μ_1 (poise)	K_1	χ_1 (Ω m)	γ (dyn cm^{-1})	$\lambda = \mu_1/\mu_2$	$q = K_1/K_2$	$R = \chi_1/\chi_2$
Polyethylene (Marlex 6009)	1.35×10^5	1×10^5	2.3	$\geqslant 10^{15}$	23.0	ca. 10^9	2.3	$\leqslant 0.3$
Nylon 12 (Hoechst)	3.5×10^4	8×10^3	16.0	ca. 4×10^{14}	23.5	ca. 10^8	16.0	$\leqslant 0.013$

[a] Phase 2 is air with $\chi_2 \approx 3 \times 10^{15}$ (Ω m).

and 1.0 cm in length (L) for polyethylene, while for nylon 12 the same L/D ratio (ca. 4.5) was maintained with $L = 1.4$ cm and $D = 0.31$ cm. The capillary served as one electrode (connected to ground) while the other was a metal plate (diameter: 8 cm) maintained perpendicular to the axis of the capillary and at a distance of 3 cm from the capillary exit. The electric field was applied across the electrodes (parallel to the direction of the central axis of the drop) from stabilized power supplies: (i) 0–15 kV ($\nu = 0$), (ii) 0–10 kV ($\nu = 60$ Hz sine wave), and (iii) 0–10 kV (ν from 0 to 7 Hz, square wave) which was obtained by connecting the dc power supply in series with a pulsed square wave. The field strength $\bar{E}_0$ expressed in kV cm^{-1} was calculated assuming that the field was uniform across the electrodes.

The deformation of the drop was recorded photographically with a motor-driven Bolex–Paillard H-16 (16 mm) ciné camera, mounted perpendicular to the field direction. A high-pressure Hg lamp served as a light source. The films were analyzed frame-by-frame by projecting the image on a transparent screen.

The deformation D_ν of the drop determined over a range of electric field strengths $\bar{E}_0$ from 0 to 5 kV cm^{-1}, is (following Torza et al.) defined as

$$D_\nu = (H - W/2)/(H + W/2) \qquad (7)$$

where H is the length of the drop measured from the exit of the capillary tube in the direction of the applied field, and W is the width of the drop at the exit of the capillary tube (see Fig. 2).

It is important to emphasize that the drop is not isolated but is suspended at the tip of the capillary; accordingly, its deformation by the electric field cannot be considered as occurring under conditions of constant volume as required by the theory. For this reason the experiments have been restricted to the small deformations attainable at low electric field strengths, for which the volume of the deformed drop does not differ markedly from the initial volume.
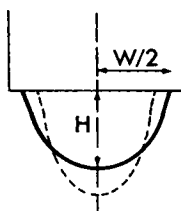

Fig. 2. Schematic representation of the deformation of the pendant drop. H and W are defined in the text.
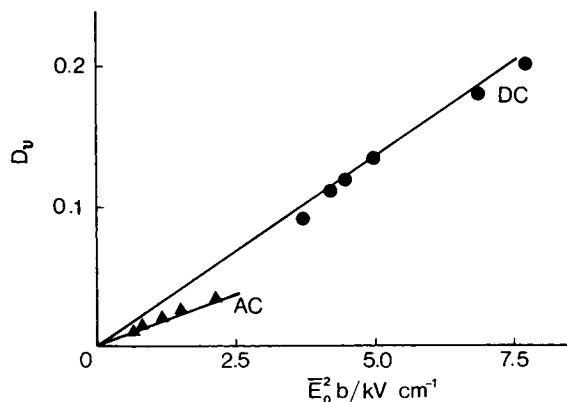
Fig. 3. Deformation of a pendant drop of polyethylene in an electric field. The positive slope indicates that the drop is deformed in the direction of the field. Circles: dc ($\nu = 0$) field with negative polarity; triangles: ac field ($\nu = 60$ Hz).

In order to interpret the experimental data in terms of the theory of Torza et al.[14] it is assumed that the pendant drop is hemispherical and that the deformation is that which would have been observed had a spherical drop been suspended in the same medium and subjected to the various fields. Furthermore, since the weight of the hemispherical drop is very small, the effect of gravity on the deformation can be neglected.

RESULTS AND DISCUSSION

Figures 3 and 4 illustrate the variation of the droplet deformation D_ν with the applied field for the two polymers studied. It is seen that over the range 0–5 kV cm^{-1} of $\overline{E}_0$, the measured values of D_0 and D_{60} showed a linear variation with
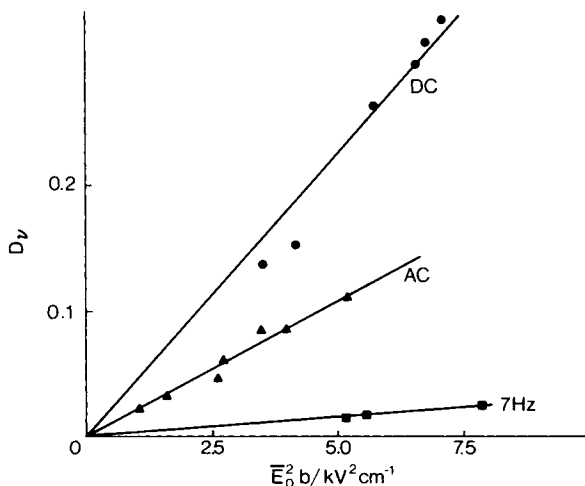

Fig. 4. Deformation of a pendant drop of nylon 12 melt in an electric field. The positive slope indicates that the drop is deformed in the direction of the electric field. Circles: deformation in a dc ($\nu = 0$) field; triangles: deformation in an ac ($\nu = 60$ Hz) field; squares: deformation in a square wave ($\nu = 7$ Hz) field.

$\bar{E}_0^2 b$ as predicted by eq. (4). From the plots shown in Figures 3 and 4, experimental values of m_ν^* were evaluated by the method of least squares. In Table II these values (m_0^* and m_{60}^*) are compared with those calculated (m_0 and m_{60}) from eq. (4).

For both polymers studied $Rq < 1$ (see Table I) and in agreement with the theoretical predictions $m_0 > m_{60} > 0$; the drop deforms into a prolate spheroid whose semimajor axis is in the direction of the field and the deformation is greater for steady ($\nu = 0$) than for alternating ($\nu = 60$ Hz) fields. Furthermore, for both polymers (m_ν^*/m_ν) > 1; this indicates that the observed deformations are greater than predicted. As indicated above, a similar discrepancy has been observed by Torza et al.,[14] especially in the case where the medium is a dielectric; they discussed a variety of explanations including the possible effects of surface conductance, electrocapillarity, and convection of charge, all of which are neglected in the theory. Recently, Ajayi[21] has reexamined the problem paying particular attention to the boundary conditions to be satisfied at the surface of the deforming drop. By satisfying these conditions more accurately than was done in previous work, an increase in drop deformation was found, which partly explains the discrepancy. In the present work with polymer melts there are two experimental factors that may contribute further to the lack of agreement between the calculated and observed deformations. First, because of the geometry of the apparatus the field intensity around the drop may be larger than the value calculated assuming homogeneity of the electric field. Second, as a first approximation, room-temperature values of the resistivities χ were used, whereas the experimental temperatures were in the vicinity of 200°C. For this reason, the values of R used in the calculations are not entirely reliable.

In spite of these uncertainties, the theory does explain qualitatively the principal experimental observations. This implies that there is no essential difference between the mechanism of the drop deformation in the case of polymeric and simple fluids. Evidently, the drop becomes charged by induction and the interaction between the field and the distribution of charge at the drop interface leads to the establishment of normal electrical stresses which, in the case of systems with $Rq < 1$, causes deformation of the drop in the direction of the field. As the field is increased, the stresses on the drop increase until the surface tension can no longer contain them. The drop then becomes unstable and jet formation occurs. The cohesion of the jet is probably aided by the low surface tension and high viscosity of the polymer melt.

The agreement between the theoretical predictions and experimental observations is surprising, since the boundary conditions in the theory do not correspond to the experiment. Nevertheless, the experiments strongly suggest that the same parameters might be involved in the two cases. In future work, it would be of interest to carry out experiments with isolated drops of a variety of molten

TABLE II
Comparison of Observed and Calculated Deformations

System	m_0 (kV^{-2} cm)	m_0^* (kV^{-2} cm)	m_0^*/m_0	m_{60} (kV^{-2} cm)	m_{60}^* (kV^{-2} cm)	m_{60}^*/m_{60}	ϕ_0	ϕ_{60}
PE–air	0.0162	0.0264	1.63	0.0020	0.0152	7.6	0.7506	0.0914
Nylon–air	0.0203	0.044	2.17	0.0147	0.0210	1.43	0.9614	0.6944

polymers in an appropriate liquid medium subjected to a well defined uniform electric field, the situation for which the theory of Torza et al.[14] was originally developed.

It has been shown above that there is qualitative agreement between the theory and experimental observations. This permits the identification of the parameters governing the deformation, and a number of interesting inferences can then be made. The parameters influencing the deformation are defined by eqs. (4) and (5). It may be noted that in the particular case of the systems studied here, where the polymer melt is essentially suspended in air, the parameter λ becomes very large and can be cancelled from the numerator and denominator in eq. (5). It follows that, for these systems, the deformation is for all practical purposes independent of λ, and the relative deformation of different polymers will be determined in large measure by their electrical properties, in particular by the parameters q and R. Of these two parameters q is probably the more important since R does not vary greatly from one polymer to another. Accordingly, it can be expected that the larger the value of q the greater will be the observed deformation. This is probably the reason why nylon 12 shows a much larger deformation than polyethylene (see Figs. 3 and 4). In this connection, an interesting polymer for further study would be poly(vinylidene fluoride), which has a dielectric constant that is approximately twice that of nylon 12. This polymer has recently attracted special attention because of its piezoelectric and pyroelectric properties.

From eq. (5), it can be expected that only those polymers for which $D_\nu > 0$ and $\phi_\nu > 0$ will be able to form fibers by deformation of the melt in an electric field. Practically all fiber-forming polymers fall into this category.

Returning to the experimental observations, it has been shown that for both polymers, polyethylene and nylon 12, the deformation in steady (dc) fields is greater than in alternating (ac) fields (see Figs. 3 and 4, and Table I). These results make it reasonable to suppose that the critical field intensity required for instability (i.e., jet formation) will be higher in ac than in dc fields.

Finally we consider briefly the role of the rheological properties of the melt in its deformation behavior. In view of the drawing nature of the induced flow, it is surprising that a theory implicitly developed for a Newtonian fluid is adequate to describe the deformation behavior of a polymer melt which is expected to exhibit non-Newtonian flow. It might be expected that the rheological properties would affect the results in the case of the oscillating field and would also affect the time to reach equilibrium in the static case. Further experimental studies would be required to assess these effects. It seems pertinent to note, however, that under the conditions used in these experiments (i.e., very low deformations) there is probably no difference between the deformation behavior of Newtonian and non-Newtonian fluids. In other words, the deformation rates are expected to be less than the average relaxation times of the fluid itself.

References

1. G. I. Taylor, *Proc. R. Soc. London, Ser. A*, **313**, 453 (1969).

2. J. Zeleny, *Phys. Rev.*, **10**, 1 (1917).

3. B. Vonnegut and R. L. Neubauer, *J. Colloid Sci.*, **7**, 616 (1952).

4. V. G. Drozin, *J. Colloid Sci.*, **10**, 158 (1955).

5. M. A. Nawab and S. G. Mason, *J. Colloid Sci.*, **13**, 179 (1958).

6. S. B. Sample and R. Bollini, *J. Colloid Interface Sci.*, **41**, 285 (1972).

7. G. I. Taylor and C. T. Wilson, *Proc. Camb. Philos. Soc.*, **22**, 728 (1925).

8. C. T. O'Konski and H. C. Thacher, *J. Phys. Chem.*, **57**, 955 (1953).

9. C. T. O'Konski and R. L. Gunther, *J. Colloid Sci.*, **10**, 563 (1955).

10. C. T. O'Konski and F. E. Harris, *J. Phys. Chem.*, **61**, 1172 (1957).

11. G. I. Taylor, *Proc. R. Soc. London, Ser. A*, **280**, 383 (1964).

12. R. S. Allan and S. G. Mason, *Proc. R. Soc. London, Ser. A*, **267**, 45 (1962).

13. L. Larrondo and R. St. John Manley, *J. Polym. Sci. Polym. Phys. Ed.*, **19**, 909 (1981), Paper I.

14. S. Torza, R. G. Cox, and S. G. Mason, *Philos. Trans. R. Soc. London, Ser. A*, **269**, 295 (1971).

15. C. Sozou, *Proc. R. Soc. London, Ser. A*, **331**, 263 (1972).

16. D. M. Taylor and T. J. Lewis, *J. Phys. D*, **4**, 1346 (1971).

17. G. A. Lushcheikin, M. K. Dobrokholova, and N. K. Treshchalina, *Sov. Plast.*, **11**, 59 (1971).

18. J. Sayers, *Proc. R. Soc. London, Ser. A*, **169**, 83 (1938).

19. H. Schonhorn, *Makromol. Chem.*, **93**, 262 (1966).

20. M. I. Kohan, *Nylon Plastics*, Interscience, New York, 1973, p. 393.

21. O. O. Ajayi, *Proc. R. Soc. London, Ser. A*, **364**, 499 (1978).